



HAL
open science

Strain sensitivity and symmetry of 2.65 eV color center in diamond nanoscale needles

Linda Venturi, Lorenzo Rigutti, Jonathan Houard, Ivan Blum, S. Malykhin,
A. Obraztsov, Angela Vella

► **To cite this version:**

Linda Venturi, Lorenzo Rigutti, Jonathan Houard, Ivan Blum, S. Malykhin, et al.. Strain sensitivity and symmetry of 2.65 eV color center in diamond nanoscale needles. Applied Physics Letters, 2019, 114 (14), pp.143104. 10.1063/1.5092329 . hal-02109311

HAL Id: hal-02109311

<https://hal.science/hal-02109311>

Submitted on 20 Jul 2020

HAL is a multi-disciplinary open access archive for the deposit and dissemination of scientific research documents, whether they are published or not. The documents may come from teaching and research institutions in France or abroad, or from public or private research centers.

L'archive ouverte pluridisciplinaire **HAL**, est destinée au dépôt et à la diffusion de documents scientifiques de niveau recherche, publiés ou non, émanant des établissements d'enseignement et de recherche français ou étrangers, des laboratoires publics ou privés.

Strain sensitivity and symmetry of 2.65 eV color center in diamond nanoscale needles

Cite as: Appl. Phys. Lett. **114**, 143104 (2019); <https://doi.org/10.1063/1.5092329>

Submitted: 10 February 2019 . Accepted: 20 March 2019 . Published Online: 11 April 2019

L. Venturi, L. Rigutti , J. Houard , I. Blum , S. Malykhin , A. Obraztsov , and A. Vella 



View Online



Export Citation



CrossMark

ARTICLES YOU MAY BE INTERESTED IN

[Nanotesla sensitivity magnetic field sensing using a compact diamond nitrogen-vacancy magnetometer](#)

Applied Physics Letters **114**, 231103 (2019); <https://doi.org/10.1063/1.5095241>

[Tin-vacancy in diamonds for luminescent thermometry](#)

Applied Physics Letters **112**, 241902 (2018); <https://doi.org/10.1063/1.5037053>

[Long optical coherence times of shallow-implanted, negatively charged silicon vacancy centers in diamond](#)

Applied Physics Letters **116**, 064001 (2020); <https://doi.org/10.1063/1.5143014>

 Measure Ready
FastHall™ Station

The highest performance tabletop system
for van der Pauw and Hall bar samples



Learn more

 Lake Shore
CRYOTRONICS

AIP
Publishing

Strain sensitivity and symmetry of 2.65 eV color center in diamond nanoscale needles

Cite as: Appl. Phys. Lett. **114**, 143104 (2019); doi: [10.1063/1.5092329](https://doi.org/10.1063/1.5092329)

Submitted: 10 February 2019 · Accepted: 20 March 2019 ·

Published Online: 11 April 2019



View Online



Export Citation



CrossMark

L. Venturi,¹ L. Rigutti,¹  J. Houard,¹  I. Blum,¹  S. Malykhin,^{2,3}  A. Obratsov,^{2,3}  and A. Vella^{1,a)} 

AFFILIATIONS

¹Groupe de Physique des Matériaux UMR CNRS 6634 – Université et INSA de ROUEN, Université Normandie, 76801 Saint Etienne Du Rouvray Cedex, France

²Department of Physics, M. V. Lomonosov Moscow State University, Moscow 119991, Russia

³Department of Physics and Mathematics, University of Eastern Finland, Joensuu 80101, Finland

^{a)}angela.vella@univ-rouen.fr

ABSTRACT

Color centers in diamond have unique applications as nanoscale field sensors. In particular, in the case of strain field, they are key components for the realization of strain-coupled hybrid spin-oscillator systems. Here, we report on the strain sensitivity of the color center emitting at 2.65 eV in diamond nanoscale needles. By contactless piezo-spectroscopy, we compare the strain sensitivity of this center with that of the well-known neutral nitrogen-vacancy (NV0) center. We demonstrate that the 2.65 eV center has a higher strain sensitivity than the NV0 center and can be explored as a strain sensor and/or for strain-coupled systems. Moreover, we perform polarization-resolved photoluminescence spectroscopy under a high uniaxial tensile stress and the polar behavior reported for the 2.65 eV center points out to a defect symmetry which is different from that of the NV0 center.

Published under license by AIP Publishing. <https://doi.org/10.1063/1.5092329>

Color centers in diamond, in particular nitrogen-vacancy (NV) centers, have been investigated for the implementation of quantum bits for quantum information processing and for the development of nanoscale electromagnetic field, temperature or pressure sensors.^{1–5} In particular, in the case of the strain field, color centers were used to assess the stress tensor through single defect spectroscopy^{3,6,7} and, inversely, the radiative optical transition of single NV defect centers could be controlled by the strain field.⁸ All these studies open the way to the realization of strain-coupled hybrid spin-oscillator systems, where the NV center spins interact with the resonant phonon modes of a macromechanical resonator through crystal strain. Such a system can lead to several applications such as cooling the mechanical resonator to a sub-thermal state.^{9–11} For all these applications, NV centers are used due to their well-known ability to couple to external strain fields.

In the present work, we focus on a color center which has its photoluminescence (PL) zero-phonon line (ZPL) at 2.65 eV (468 nm) whose nature is not yet clear according to the literature.¹² This defect could correspond to TR12' (ZPL ranging between 2.648 and 2.654 eV). It was labeled as TR12' because it is 10 meV blue-shifted to the TR12 color center.^{13–15} The 2.65 eV center was observed on most of the as-grown chemical vapor deposition (CVD) diamond films studied by Iakoubovskii and Adriaenssens¹⁵ Unlike the TR12 center which

anneals out at 800 °C, the intensity of the 2.65 eV center was almost constant in CVD films grown annealed up to 1000 °C.¹⁶

The TR12 center was observed in the PL spectrum of diamond decades ago and Davies *et al.*¹⁷ performed accurate piezo-spectroscopic studies on it, in order to determine the strain susceptibility and the symmetry of this center. They measured a strain susceptibility (sensitivity) lower than that of the NV0 center and they were unable to establish the symmetry of the center.¹⁷ Concerning its structure, Mainwood *et al.*¹⁸ proposed that this center contains an interstitial carbon in a hexagonal site. Recently, Naydenov *et al.*¹⁹ have demonstrated the ability of the TR12 center as a single photon emitter, once again fueling interest in this color center and the related TR12' or 2.65 eV center.

Concerning the 2.65 eV center, Iakoubovskii and Adriaenssens¹⁵ suggested that it is a stressed TR12 center, with the stress being generated through the lattice or some neighboring impurity. However, the structure and symmetry of this center are not well-known and its potential as a sensor was never tested.^{16,17,20}

Here, using an original method to perform contactless piezo-spectroscopy on a nanoscale needle-shaped specimen,²¹ we prove that 2.65 eV centers present a higher sensitivity to the strain field compared to the NV0 center. Therefore, this color center seems a better candidate for the fabrication of strain-mediated coupling systems. Moreover, we

TABLE I. Geometrical parameters of the analyzed diamond needles.

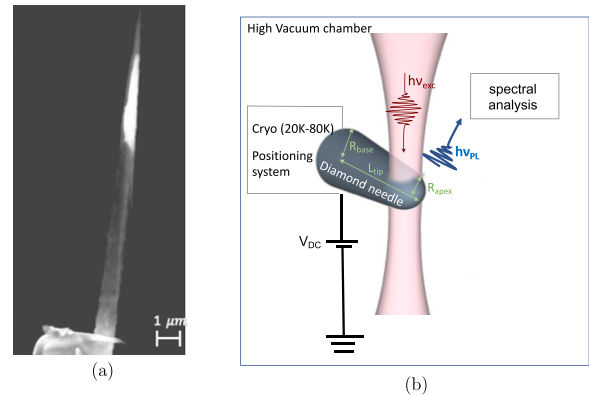
Needle specimen	Apex radius R_{apex} (nm)	Base radius R_{base} (nm)	Length L_{tip} (μm)
Tip 1	71	500	21
Tip 2	150	1800	40

performed polarization-resolved micro-PL under strain field to obtain more information on the symmetry and structure of the 2.65 eV (TR12') center.

We perform contactless piezo-spectroscopy on diamond nanoscale needles. These single crystal needles are obtained by a combination of chemical vapor deposition (CVD) and selective oxidation of polycrystalline carbon films. The diamond needles are oriented along the $\langle 001 \rangle$ crystallographic direction. More information on the sample synthesis is presented in Ref. 22. A large number of needles was scattered on a silicon substrate, individual needles were selected and glued on an electro-polished tungsten tip by micromanipulation under an optical microscope. The exact geometry of the samples, measured with scanning electron microscopy (SEM), is reported in Table I, for the two samples analyzed in this work. The SEM image of Tip 1 is reported in Fig. 1(a).

Experiments are performed at 25 K under ultrahigh vacuum conditions ($< 10^{-7}$ Pa). A high voltage of several kilovolts is applied to the tungsten tip and produces an intense electric field at the apex of the diamond needle, as experimentally and theoretically proved by authors in Refs. 21 and 23.

The PL signal of the diamond needles is excited by a linearly polarized laser beam of 150 fs pulse duration at 260 nm, at a frequency of 500 kHz and an average power of 400 μW . The laser beam waist, focused by a spherical mirror on the tip specimen, is about 1.5 μm . The position of the specimen is controlled by a closed feedback loop three-axial piezoelectric stage. The PL signal is collected and analyzed through a grating spectrometer with 320 mm focal length and with the

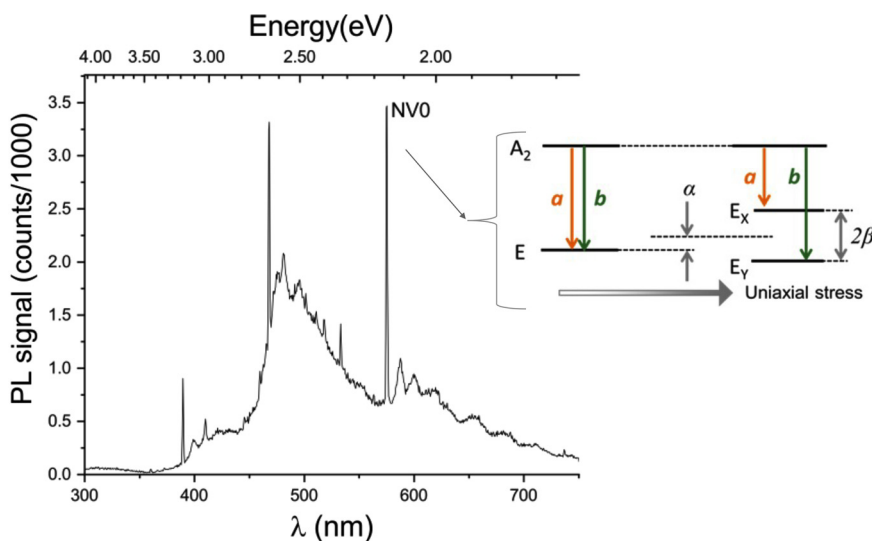
**FIG. 1.** (a) SEM image of the diamond nanoneedles (Tip1) glued on the tungsten tip. (b) Schematic of the experimental setup: cryo: cryostat.

highest spectral resolution of around 0.5 meV, equipped with a liquid nitrogen-cooled CCD camera.

A schematic of the experiment setup is reported in Fig. 1(b).

A typical μPL spectrum obtained with the laser spot positioned on the shank of needle 2 at several microns below its apex and without bias is shown in Fig. 2. In the spectrum, it is possible to recognize the emission of several types of color centers, constituted by a ZPL at a given energy and vibronic replicas.²⁴ Among these centers, the well-known neutral nitrogen-vacancy complex (NV0), exhibiting a ZPL at 2.156 eV,^{25,26} for which the electronic states and their modification under uniaxial stress are reported in the inset of Fig. 2. We can notice that the ZPL of the 2.65 eV center has almost the same intensity as the NV0 center.

The piezo-spectroscopy of the 2.65 eV center was performed as follows. A series of PL spectra was acquired for the 2.65 eV center and the NV0 center with the laser spot focused on the apex of needle 1 for different values of the applied bias, from 0 kV to 16 kV. These spectra are reported in Figs. 3(a) and 3(b); the spectra of the NV0 center are shown in parallel for comparison.

**FIG. 2.** PL signal of the diamond needle: several types of color centers can be identified; among them, the NV0 complex and the 2.65 eV center on which this study focuses. The inset shows schematic of the energy levels of the NV0 center, illustrating the effect of the uniaxial stress on the different states.

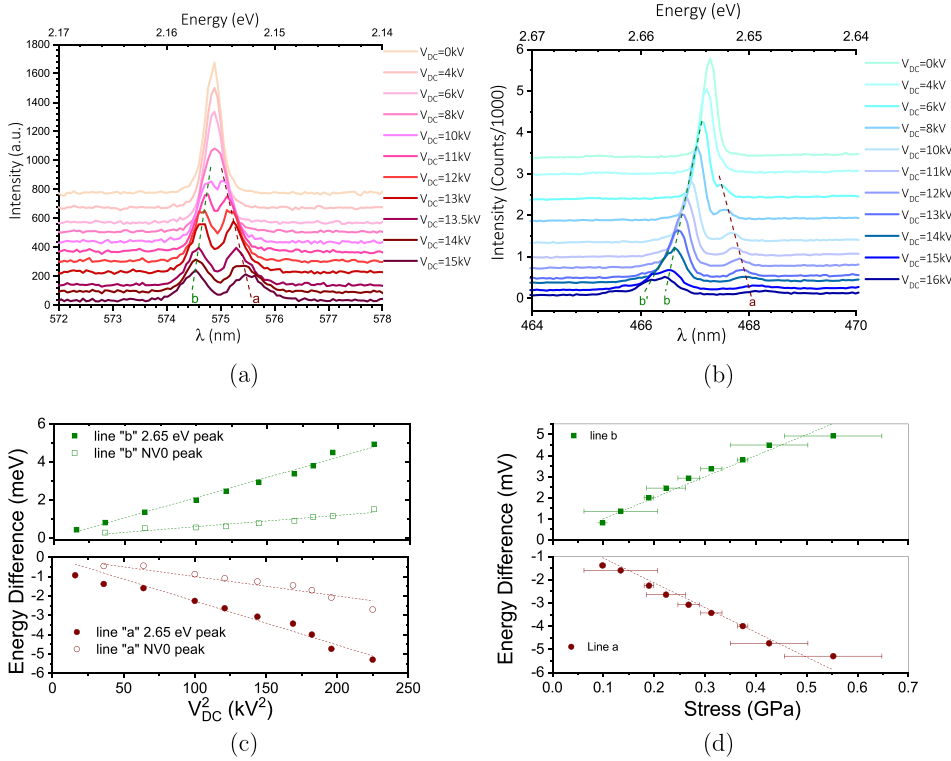


FIG. 3. Micro-PL signal from the NV0 ZPL (a) and the 2.65 eV ZPL (b) acquired with the laser impinging on the apex of needle 1 for different voltages applied to the needle, the different spectra being vertically shifted for clarity. The line splits up into two main components, labeled as a and b. The dashed lines are guides to the eye. (c) Dependence of the energy splitting of the a and b components on the square of the applied voltage, collected from the apex of Tip 1. (d) Dependence of the energy splitting of the a and b components of the 2.65 eV center with the stress along the needle axis ((001) crystal direction).

The spectra of both centers at a low bias consist, within the 1 meV spectral resolution limit of the setup, of single emission lines peaked at $E = 2.654$ eV and $E = 2.156$ eV, respectively. At higher biases, this line splits into two components, denoted as a and b, which shift towards lower and higher energies, respectively, as the bias is increased. As it was recently proved in Ref. 21, the application of a bias of several kilovolts to diamond needles having nanometric transverse dimensions produces a tensile uniaxial stress within the needles. The relationship between the applied voltage and the uniaxial stress (along the z direction, which corresponds to the tip axis) is

$$\sigma_{zz}(z) = \frac{\pi R_{apex}^2 \sigma_{apex}}{S(z)}, \quad (1)$$

where $S(z) = \pi(R_{apex} + \frac{(R_{base} - R_{apex})z}{L_{tip}})^2$ is the area of the axial cross section at the coordinate z, for a circular cone geometry, R_{apex} , R_{base} and L_{tip} are the geometrical parameters of the tip, defined in Fig. 1(b) and in Table I, and σ_{apex} is the field-induced-Maxwell stress given by

$$\sigma_{apex} = \frac{1}{2} \epsilon_0 F_s^2 = \frac{1}{2} \epsilon_0 \left(\frac{V_{DC}}{k_f R_{apex}} \right)^2, \quad (2)$$

where k_f is a geometrical factor depending on the tip geometry and electrostatic environment of the tip.²⁷

For the NV0 center, the uniaxial stress induces splitting of the E state into two branch states E_x and E_y , as illustrated in the inset of Fig. 4. Therefore, the a and b lines correspond to $A_2 \rightarrow E_x$ and $A_2 \rightarrow E_y$ transitions, respectively, and they have almost the same amplitude.^{8,26} However, for the 2.65 eV center, the b line has a higher intensity than the a line suggesting a different transition

probability toward the two perturbed electronic states. Moreover, at high biases, a new line b' is visible, but not an a' line, because, due to its lower intensity, it is masked by the noise level. We attribute the b and b' components to two different centers, simultaneously excited by the laser beam but because they are probably at

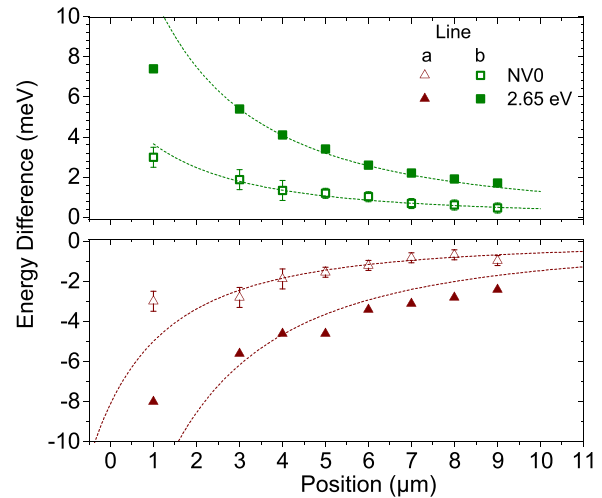


FIG. 4. Energy splitting (left-hand side ordinates) of NV0 and 2.65 eV components a (bottom) and b (top) and related uniaxial stress along (100) (right-hand side ordinates) as a function of the position along the needle axis. The fit of the experimental data yields a value for the stress at the apex.

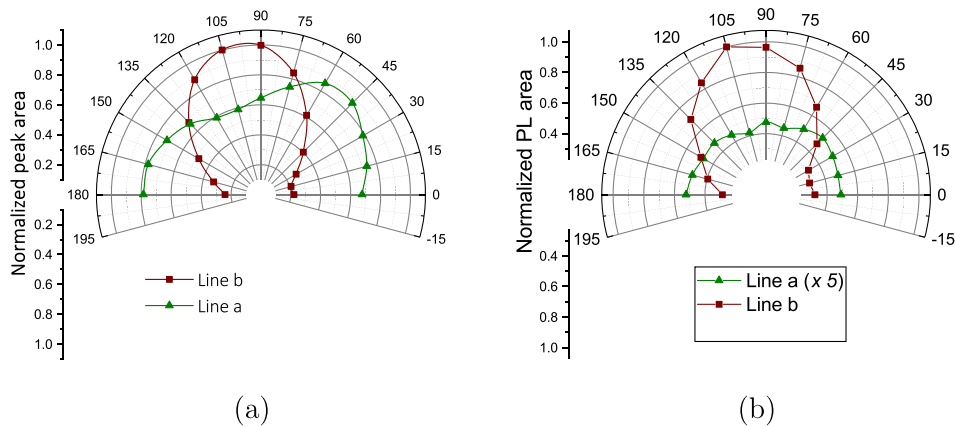


FIG. 5. Polarization-resolved analysis of the NV0 ZPL (a) and the 2.65 eV peak (b) acquired on the apex of needle 1 at $V_{DC} = 16$ kV.

different positions inside the illuminated zone, they will be subjected to a slightly different perturbation.²¹ For both centers, the energy splitting of the a and b components is a quadratic function of the applied bias, and, following Eqs. (1) and (2), a linear function of the uniaxial tensile stress regime along the $\langle 001 \rangle$ direction. For the NV0 center the relation is

$$\Delta E_{a,b} = c_{a,b} \sigma_{zz}, \quad (3)$$

with $c_a = -4.5$ meV/GPa, $c_b = 3.0$ meV/GPa.⁸ Therefore, the measurement of $\Delta E_{a,b}$ can be used to calibrate the tensile stress at a given position z within the diamond needle, as a function of the applied bias. The mean uniaxial tensile stress varies from 0 to 0.6 GPa. For each value of the bias, the range of the corresponding uniaxial tensile stress is reported as an error bar in Fig. 3(d). The values of $\Delta E'_{a,b}$ measured for the 2.65 eV center are reported as a function of the stress in Fig. 3(d); they show a linear behavior as a function of the applied tensile stress

$$\Delta E'_{a,b} = k_{a,b} \sigma_{zz}. \quad (4)$$

The proportionality coefficients $k_a = -(10.7 \pm 0.3)$ meV/GPa and $k_b = (10.0 \pm 0.3)$ meV/GPa are obtained by a linear fit of data reported Fig. 3(d). Their values are larger than the values of the $c_{a,b}$ coefficients of the NV0 center, by more than a factor 2. This method does not exclude systematic errors which could arise when single color centers close to the tip apex are excited. In fact, a difference in the position of the NV0 or 2.65 eV center could translate into a significantly different stress state acting on one or the other.

For this reason, spatially resolved PL measurements were performed on Tip 2. The PL spectra were acquired at different positions of the laser spot with respect to the apex of needle 2, subjected to a bias $V_{DC} = 16$ kV. When the laser is focused close to the apex of the needle, the ZPL of NV0 and 2.65 eV peaks splits up into different components, similarly to the dataset shown in Figs. 1(a) and 1(b). The energy difference for the two centers is plotted as a function of the laser spot position with respect to the apex of the needle in Fig. 4. This complementary method averages out the possible biases induced by the measurement performed at the apex only, so that the stress felt by NV0 is, on the average, the same felt by the 2.65 eV center along the needle length.

In the case of the NV0 center, the energy difference $\Delta E_{a,b}$ is higher than 1 meV up to a position of $4 \mu\text{m}$ from the apex, but it

progressively decreases to zero. A similar behavior was reported for the 2.65 eV center, even though the spectral shift is higher than 2 meV up to the furthest position of $10 \mu\text{m}$. The experimental data have been fitted using Eq. (1). The results yield the value of apex stress $\sigma_{apex} = (1.8 \pm 0.3)$ GPa, and the value of the stress at each z position.

Therefore, the values of energy difference $\Delta E'_{a,b}$ of the 2.65 eV peak can be associated with the corresponding values of the uniaxial tensile stress. Using Eq. (4), the values of $k_a = -(11 \pm 1)$ meV/GPa and $k_b = (10.0 \pm 0.5)$ meV/GPa are obtained. These values are in agreement with the values obtained on needle 1 when varying the applied bias, also showing that the previous method did not yield a biased value.

In order to obtain more information on the symmetry of this center, polarization-resolved PL spectroscopy was performed on needle 1, while it is subjected to a bias $V_{DC} = 16$ kV (Fig. 5).

The polar representation of the area of the two components a and b of the NV0 ZPL shows a trigonal symmetry with the intensity of the b(a) line exhibiting a minimum (maximum) at 0° and 180° (π polarization) and a maximum (minimum) at 90° (σ polarization) [Fig. 5(a)]. The intensity ratio b/a is equal to 0.46 in π polarization and 3.5 in σ polarization, which is close to the literature values of 0 (π) and 3 (σ), respectively.⁸ In the case of the 2.65 eV peak, the b line shows the same polarization behavior as the b line of the NV0 center, however, as already discussed, its intensity is higher than the intensity of the a line by almost a factor of 10. This line of the 2.65 eV center shows an increase in intensity of about 10% in π polarization, compared to σ polarization [Fig. 5(b)]. Also, even though the polar behaviors of the a and b lines of the 2.65 eV center are similar to those of the split components of the NV0, the intensity ratio (b/a) is 3 in π polarization and 10 in σ polarization, which is incompatible with the monoclinic I or the triclinic symmetry proposed in the literature for TR12 and TR12' centers.^{16,17,20}

In summary, we have performed contactless piezo-spectroscopy of the 2.65 eV center on a diamond needle-shaped crystal with a nanometric apex radius and with axis oriented along the $\langle 001 \rangle$ crystal direction. The PL signal related to the ZPL of this color center exhibits an energy splitting scaling linearly with the uniaxial tensile stress along the $\langle 001 \rangle$ direction. This splitting was compared to the splitting reported on the well-known NV0 center. For the same value of the stress, the splitting of the 2.65 eV center is twice as large as that of the NV0 center. This result was reproduced on several samples and reported here for two samples having different geometries. Moreover, this result was

obtained using two different methodologies to vary the applied uniaxial tensile stress (variation of the bias or the laser spot position along the needle). We also performed polarization-resolved PL spectroscopy on the 2.65 eV center. Despite this complete piezo-spectroscopy study, varying the direction of the tensile stress would still be necessary to obtain an unambiguous picture of the symmetry of this center, which could ascertain that this defect does not have monoclinic I or trigonal symmetry. This difference in symmetry with respect to NV0 centers could partly explain its extreme strain sensitivity. We notice that this color center can be easily included in the needle-shape nanoscale system; this could make it a valid alternative to the NV-type centers, if a suitable strategy for the control of its density is developed, in the framework of nanoscale probes of electromagnetic fields.

This work was supported by the European Union with the European Regional Development Fund (ERDF) and the Regional Council of Normandie and by the Carnot Institut ESP and Russian Foundation for Basic Research (Grant No. RFBR 18-02-00495).

REFERENCES

- ¹L. Childress and R. Hanson, *MRS Bull.* **38**, 134 (2013).
- ²L. Rondin, J. Tetienne, T. Hingant, J. Roch, P. Maletinsky, and V. Jacques, *Rep. Prog. Phys.* **77**, 056503 (2014).
- ³F. Grazioso, B. R. Patton, P. Delaney, M. L. Markham, D. J. Twitchen, and J. M. Smith, *Appl. Phys. Lett.* **103**, 101905 (2013).
- ⁴A. Jenkins, M. Pelliccione, G. Yu, X. Ma, X. Li, K. L. Wang, and A. C. B. Jayich, preprint [arXiv:1812.01764](https://arxiv.org/abs/1812.01764) (2018).
- ⁵J. V. Cady, O. Michel, K. W. Lee, R. N. Patel, C. J. Sarabalis, A. H. Safavi-Naeni, and A. C. B. Jayich, preprint [arXiv:1811.04275](https://arxiv.org/abs/1811.04275) (2018).
- ⁶D. Lee, K. W. Lee, J. V. Cady, P. Ovartchayapong, and A. C. B. Jayich, *J. Opt.* **19**, 033001 (2017).
- ⁷M. E. Trusheim and D. Englund, *New J. Phys.* **18**, 123023 (2016).
- ⁸G. Davies, *J. Phys. C: Solid State Phys.* **12**, 2551 (1979).
- ⁹J. Teissier, A. Barfuss, P. Appel, E. Neu, and P. Maletinsky, *Phys. Rev. Lett.* **113**, 020503 (2014).
- ¹⁰P. Ovartchayapong, K. W. Lee, B. A. Myers, and A. C. B. Jayich, *Nat. Commun.* **5**, 4429 (2014).
- ¹¹E. MacQuarrie, M. Otten, S. Gray, and G. Fuchs, *Nat. Commun.* **8**, 14358 (2017).
- ¹²K. Iakoubovskii and A. Stesmans, *J. Phys.: Condens. Matter* **14**, R467 (2002).
- ¹³K. Iakoubovskii and G. Adriaenssens, *Phys. Rev. B* **61**, 10174 (2000).
- ¹⁴E. Rzepka, F. Silva, A. Lussion, A. Riviere, and A. Gicquel, *Diamond Relat. Mater.* **10**, 542 (2001).
- ¹⁵K. Iakoubovskii and G. Adriaenssens, *Phys. Status Solidi A* **181**, 59 (2000).
- ¹⁶K. Iakoubovskii, G. Adriaenssens, N. Dogadkin, and A. Shiryayev, *Diamond Relat. Mater.* **10**, 18 (2001).
- ¹⁷G. Davies, C. Foy, and K. ÓDonnell, *J. Phys. C: Solid State Phys.* **14**, 4153 (1981).
- ¹⁸A. Mainwood, A. T. Collins, and P. Woad, in *Materials Science Forum* (Trans Tech Publications, 1994), Vol. 143, pp. 29–34.
- ¹⁹B. Naydenov, R. Kolesov, A. Batalov, J. Meijer, S. Pezzagna, D. Rogalla, F. Jelezko, and J. Wrachtrup, *Appl. Phys. Lett.* **95**, 181109 (2009).
- ²⁰J. Walker, *J. Phys. C: Solid State Phys.* **10**, 3031 (1977).
- ²¹L. Rigutti, L. Venturi, J. Houard, A. Normand, E. P. Silaeva, M. Borz, S. A. Malykhin, A. N. Obraztsov, and A. Vella, *Nano Lett.* **17**, 7401–7409 (2017).
- ²²A. Zolotukhin, P. G. Kopylov, R. R. Ismagilov, and A. N. Obraztsov, *Diamond Relat. Mater.* **19**, 1007 (2010).
- ²³E. Silaeva, L. Arnoldi, M. Karahka, B. Deconihout, A. Menand, H. Kreuzer, and A. Vella, *Nano Lett.* **14**, 6066 (2014).
- ²⁴A. M. Zaitsev, *Optical Properties of Diamond: A Data Handbook* (Springer Science & Business Media, 2013).
- ²⁵Y. Mita, *Phys. Rev. B* **53**, 11360 (1996).
- ²⁶M. W. Doherty, N. B. Manson, P. Delaney, F. Jelezko, J. Wrachtrup, and L. C. Hollenberg, *Phys. Rep.* **528**, 1 (2013).
- ²⁷F. Vurpillot, in *Atom Probe Tomography*, edited by W. Lefebvre-Ulrikson, F. Vurpillot, and X. Sauvage (Academic Press, 2016), pp. 17–72.